

Photochemistry of Enzyme-Bound Cinnamoyl Derivatives

Paula M. Koenigs,[†] Bruce C. Faust,[‡] and Ned A. Porter^{*†}

Contribution from the Department of Chemistry and the School of the Environment, Duke University, Durham, North Carolina 27708

Received April 7, 1993[⊗]

Abstract: *p*-(Diethylamino)-*o*-hydroxy- α -methylcinnamoyl (CINN) was used as an acylating moiety for the formation of stable CINN-enzymes at the active site serine residues of the enzymes chymotrypsin, Factor Xa, and thrombin. Photolysis of the stable CINN-enzymes generates enzymatic activity *via* the proposed consecutive steps of photoisomerization (rate-determining step) and thermal lactonization (fast). Photochemical studies were undertaken to assess how an enzyme active site could alter the photochemistry of the cinnamoyl derivative. Quantum yields for *E* to *Z* photoisomerization ($\Phi_{E \rightarrow Z}$) were measured for the three CINN-enzymes at 366 nm (20 °C in pH 7.4 Tris buffer) and for the model system ethyl *p*-(diethylamino)-*o*-hydroxy- α -methylcinnamate (CINN-OEt). Relative to the value of $\Phi_{E \rightarrow Z} = 0.13$ for CINN-OEt, CINN actually displayed an enhanced isomerization efficiency while bound at the active sites of chymotrypsin and Factor Xa ($\Phi_{E \rightarrow Z} = 0.17$ and 0.23, respectively) and a decreased isomerization efficiency ($\Phi_{E \rightarrow Z} = 0.04$) while bound to thrombin. The influence of chymotrypsin's active site on cinnamoyl photoisomerization was investigated further by measuring the photostationary state isomeric ratios for MeCINN-chymotrypsin and MeCINN-OEt, the methyl ether analogue of the corresponding CINN photolytes, in pH 7.4 Tris buffer. MeCINN-chymotrypsin displayed a value of 2.7 for $\Phi_{Z \rightarrow E}/\Phi_{E \rightarrow Z}$ ($\Phi_{E \rightarrow Z}$ = quantum yield for *E* to *Z* and $\Phi_{Z \rightarrow E}$ = quantum yield for *Z* to *E*), and MeCINN-OEt exhibited a value of 1.7. This difference could not be attributed to the greater hydrophobicity of chymotrypsin's active site since values of $\Phi_{Z \rightarrow E}/\Phi_{E \rightarrow Z}$ for MeCINN-OEt in organic solvents were less than unity. Photoisomerization quantum yields were also measured for the isomers of MeCINN-chymotrypsin and MeCINN-OEt. Both acyl-enzyme isomers exhibited less efficient photoisomerization (*E* to *Z* and *Z* to *E*) than their respective model system, MeCINN-OEt.

The photocontrol of biological activity, particularly that of enzymatic activity, has been the subject of extensive recent investigation.¹ Since photoresponses *in vivo* are ultimately manifested by some enzymatic reaction, *in vitro* photocontrol of enzymatic activity can serve as a model for biological phenomena. Additionally, enzymatic photoactivation is a means of photoreleasing an active catalyst that can theoretically turn over *ad infinitum* at the expense of one photon. This methodology has perhaps been most extensively applied to the development of enzyme-based photographic systems,² but it could also potentially be used for therapeutic and diagnostic applications.³ Nature has often relied on a photochromic effector molecule interacting with a protein to control enzyme activity. In the visual process, for example, a double-bond photoisomerization of a small effector molecule is used to elicit the photoresponse.¹ Double-bond photoisomerization has likewise been used in the development of artificial photoresponsive systems.

An effector molecule being used to control enzyme activity can exert its influences either from a position remote from the active site by inducing conformational changes in the protein or at the active site by blocking essential functionality for catalysis or binding. Of this latter category, photochromic differentiation has been displayed both for competitive inhibitors and for covalently modifying inhibitors. A useful photoregulatory option arises if one state of a photochromically modified enzyme remains inhibited indefinitely but a second state quickly reverts to a fully functioning enzyme. Although this type of photoregulation is

not reversible, it does ensure a dramatic, photoinduced increase in enzymatic activity. Martinek *et al.*⁴ pioneered the use of this methodology by utilizing cinnamate photoisomerization.

Although there are many examples of cinnamoyl derivatives being used as effector moieties for enzymatic photoactivation, the successes of these attempts are widely varied depending on the particular system under investigation. For example, (*cis*-*p*-nitrocinnamoyl)chymotrypsin was ~1000 times more stable to hydrolysis than the *trans* acyl-enzyme; thus, *cis* to *trans* photoisomerization of the acyl-enzyme provided a means of enzymatic photoactivation.^{5,6} However, for (*p*-(*N,N,N*-trimethylamino)cinnamoyl)trypsin, the *trans* isomer rather than the *cis* isomer was more stable to hydrolysis by a factor of 10. Other⁷⁻¹¹ recent reports of strategies for photocontrol of enzyme activity have appeared, but quantitative data about photoefficiencies have not been reported.

For all the cases of cinnamate-enzyme inhibition reported prior to 1987, the differential reactivity of the *cis* and *trans* isomers arose solely from the unique steric demands of each isomer in the active site environment. The consequential disposition of a photoisomer in the active site determined its susceptibility to hydrolysis. This methodology had to be tailored to each new enzyme system because the success of the methodology depended upon the enzyme's ability to impart differential reactivity to the geometric isomers. Nevertheless, the use of cinnamoyl-modified

(4) Martinek, K.; Varfolomeyev, S. D.; Berezin, I. V. *Eur. J. Biochem.* 1971, 19, 242.

(5) Aisina, R. B.; Vasil'eva, T. E.; Kazanskaya, N. F.; Tikhodeeva, A. S.; Berezin, I. V. *Biokhimiya* 1973, 38, 601.

(6) (a) Kost, O. A.; Kazanskaya, N. F. *Bioorg. Khim.* 1979, 5, 1102. (b) Kost, O. A.; Kazanskaya, N. F.; Rudenskaya, G. N. *Bioorg. Khim.* 1980, 6, 1813.

(7) Harada, M.; Sisido, M.; Hirose, J.; Nakanishi, M. *FEBS Lett.* 1991, 286, 6.

(8) Willner, I.; Rubin, S. *J. Am. Chem. Soc.* 1992, 113, 3321.

(9) Willner, I.; Rubin, S. *J. Am. Chem. Soc.* 1992, 114, 3150.

(10) Kaufman, H.; Vratsanos, S. M.; Erlanger, B. F. *Science* 1968, 162, 1487.

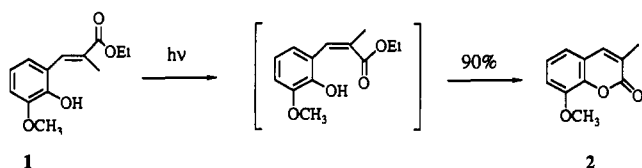
(11) Mendel, D.; Ellman, J. A.; Schultz, P. G. *J. Am. Chem. Soc.* 1991, 113, 2758.

[†] Department of Chemistry.

[‡] School of the Environment.

[⊗] Abstract published in *Advance ACS Abstracts*, September 15, 1993.

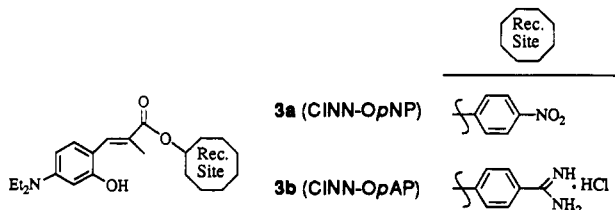
(1) Martinek, K.; Berezin, I. V. *Photochem. Photobiol.* 1979, 29, 637.
 (2) (a) Berezin, I. V.; Kazanskaya, N. F.; Aisina, R. B.; Lukasheva, E. V. *Enzyme Microb. Technol.* 1980, 2, 150. (b) Aisina, R. B.; Ereemeev, N. L.; Kazanskaya, N. F.; Ludasheva, E. V. *Biokhimiya* 1981, 46, 979. (c) Kuan, K.; Lee, Y. Y.; Tebbetts, L.; Melius, P. *Biotechnol. Bioeng.* 1979, 21, 443.
 (d) Kuan, K. N.; Lee, Y. Y. *Biotechnol. Bioeng.* 1980, 22, 1725.
 (3) (a) Pizzo, S. V.; Turner, A. D.; Porter, N. A.; Gonias, S. L. *Thromb. Haemostasis* 1986, 56, 387. (b) Porter, N. A.; Bruhnke, J. D. *Photochem. Photobiol.* 1990, 51, 37.

Scheme I. Photochemical Synthesis of a 3-Methylcoumarin Derivative, Photoisomerization Followed by Cyclization

enzymes had proven to be a useful approach to the photoactivation of several serine proteases.

Turner *et al.*¹² employed a strategy in which differential reactivity was intrinsic to a pair of cinnamoyl geometric isomers. An *E* to *Z* photoisomerization was used to place an internal nucleophile in proximity to the cinnamoyl carbonyl whereby deacylation could occur *via* cyclization. This strategy was based on a photochemical synthesis of 3-methylcoumarins.¹³ Photolysis of **1** produced **2** in high yield, presumably by effecting an *E* to *Z* isomerization whereby the ester linkage became accessible to the nucleophilic *o*-hydroxyl (Scheme I). Lactonization is apparently fast since the effective molarity for the cyclization of *cis*-cinnamic acid is 3.7×10^{11} relative to the esterification of acetic acid with ethanol.¹⁴

The *p*-diethylamino derivatives **3a** and **3b** have proved to be useful for fulfilling an enzyme inhibition–photoactivation scheme.¹⁵ The ester linkage was used to introduce functionality into the cinnamate derivative which would serve as the recognition site (Rec. Site) for an enzyme being targeted for inhibition. Thus,



3a was used as a chymotrypsin inhibitor since *p*-nitrophenyl (*p*NP) mimics the aromatic, hydrophobic side chains for which chymotrypsin is specific, and **3b** was used as an inhibitor for thrombin and Factor Xa since the *p*-amidinophenyl (*p*AP) resembles the positively charged P₁ side chains of lysine and arginine for which these enzymes are specific. CINN-OpNP and CINN-OpAP are inverse inhibitors (irreversible inhibitors having the recognition site on the leaving group).¹⁶ Reaction with inverse inhibitors is a general method by which the same acyl derivative can be introduced into many different active site environments.

When a particular serine protease is reacted with its inhibitor, CINN-OpNP or CINN-OpAP, the catalytically active serine residue becomes acylated (Scheme IIa). A crystal structure has been solved for the chymotrypsin-derived acyl-enzyme¹⁷ CINN-chymotrypsin, providing structural evidence that Ser 195 of the active site is the point of attachment for the acylating moiety. Contrary to the endogenous mechanism of serine protease hydrolysis in which the intermediate acyl-enzymes are quickly attacked by water, the CINN-enzymes which are derived from chymotrypsin, Factor Xa, and thrombin are very stable to hydrolysis.

(12) (a) Turner, A. D.; Pizzo, S. V.; Rozakis, G.; Porter, N. A. *J. Am. Chem. Soc.* **1988**, *110*, 244. (b) Turner, A. D.; Pizzo, S. V.; Rozakis, G.; Porter, N. A. *J. Am. Chem. Soc.* **1987**, *109*, 1274.

(13) Mali, R. S.; Yeola, S. N.; Kulkarni, B. K. *Indian J. Chem.* **1983**, *22B*, 352.

(14) Gerstein, J.; Jencks, W. P. *J. Am. Chem. Soc.* **1964**, *86*, 4655. Effective molarity is defined as the concentration of an external nucleophile required to give a reaction rate equal to the reaction rate of the comparable internal nucleophile.

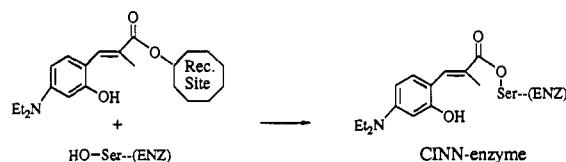
(15) Bruhnke, J. B. Ph.D. Dissertation, Duke University, 1990.

(16) Tanizawa, K.; Kanaoka, Y. In *Topics in Current Chemistry*; Vogtle, F., Weber, E., Eds.; Springer-Verlag: Berlin, 1986; Vol. 136, pp 81–107.

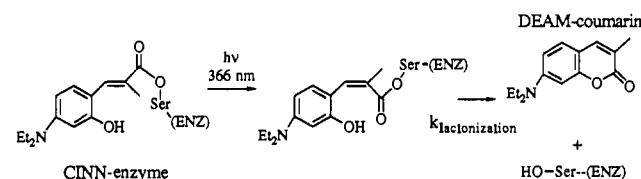
(17) Stoddard, B. L.; Bruhnke, J.; Porter, N.; Ringe, D.; Petsko, G. A. *Biochemistry* **1990**, *29*, 4871.

Scheme II. Serine Protease Inhibition–Photoactivation Scheme for (*E*)-*p*-(Diethylamino)-*o*-hydroxy- α -methylcinnamate Ester Inhibitors

a. Inhibition

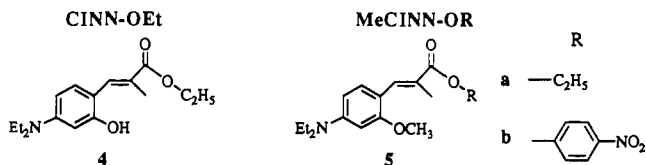


b. Photoactivation



Despite the importance of having an efficient photochemical step to achieve effective enzymatic activation, no quantitative information has been collected for the photoefficiencies of activation for these types of systems. The crystal structure of CINN-chymotrypsin indicates that the conjugated system of the photochromic moiety lies flat within the primary binding pocket of chymotrypsin,¹⁷ being surrounded on both faces by atoms of the peptide backbone. Several van der Waals contacts exist between the π electron cloud and the main-chain atoms with interatomic distances varying between 3.1 and 3.9 Å.¹⁷ This illustrates that within the active site, an isomerizing cinnamoyl will have to contend with very different environmental factors as compared to when it undergoes this transformation as a cinnamate derivative in bulk solvent.

In order to provide some quantitative data about photoisomerization of enzyme-bound substrates, we have determined quantum yields for cinnamate-modified enzymes. Initially, quantum yields of photoactivation were determined for the three CINN-enzymes of chymotrypsin, Factor Xa, and thrombin. The results were compared to the quantum yields measured for a model system, ethyl (*E*)-*p*-(diethylamino)-*o*-hydroxy- α -methylcinnamate (CINN-OEt), **4**. Chymotrypsin was also acylated by the *E* and *Z* isomers of MeCINN *via* enzymatic reaction with (*E*)- or (*Z*)-**5b**.



Photostationary state (PSS) experiments on these systems and on the model systems (*E*)-**5a** and (*Z*)-**5a** allowed us to examine the effect of chymotrypsin's active site on both an *E* to *Z* and a *Z* to *E* photoisomerization.

Experimental Section

Chromogenic Assays of Enzymatic Activity-Reagents and Materials. Except as noted, all solvents and reagents were reagent grade and used directly as received (Aldrich, Milwaukee, WI). Tetrahydrofuran was distilled from sodium/benzophenone ketyl immediately prior to use. *N,N*-dimethylformamide (DMF) was glass-distilled and stored over 4-Å molecular sieves. Pyridine was distilled from calcium hydride and stored over potassium hydroxide. Compounds **4**, **3a**, and **3b** were synthesized according to established procedures.^{3b,15}

Chymotrypsin and thrombin were purchased from Sigma Chemical Co. Type 1-S α -chymotrypsin from bovine pancreas was utilized. It had

a specific activity of 50 units/mg protein¹⁸ as determined by assay with benzoyl-L-Tyr ethyl ester. Human thrombin was utilized which had a specific activity of ~1000 NIH units/mg protein. Bovine Factor Xa (Enzyme Research Laboratories) was utilized which had a specific activity of 269 units/mg protein²⁰ as determined by assay with chromogenic substrate CBS 31.39 as supplied by Diagnostica Stage (France).

Bovine serum albumin (BSA) was purchased from Sigma Chemical Co. Sephadex G-25 was supplied by Pharmacia Fine Chemicals. Disposable gel filtration columns were purchased from Kontes Scientific Glassware. Milllex-GV syringe filter units with 0.22- μ m Durapore membranes were obtained from Millipore Corp. Disposable, semimicro methacrylate or polystyrene cuvettes were purchased from Dynalab Corp. Buffers were prepared with tris(hydroxymethyl)aminomethane (Tris) (ultra pure) from Schwarz/Mann Biotech, CaCl₂ from J. T. Baker Chemical Co., and NaCl (analytical reagent) from Mallinckrodt, Inc. The chromogenic assay substrates S-2586, S-2222, and S-2238 were obtained from Kabi-Vitrum.

Chymotrypsin activity was assayed in a buffer of 30 mM Tris, 400 mM NaCl, and 3 mM CaCl₂, pH 8.3, and activity for thrombin and Factor Xa was measured in a buffer of 50 mM Tris and 250 mM NaCl, pH 8.3. For all purposes other than the enzymatic assays, a buffer of 50 mM Tris and 150 mM NaCl with an adjustment to pH 7.4 with HCl was used.

Standard ferrioxalate actinometry was used.^{19,20} The actinometer solution was prepared with anhydrous Fe₂(SO₄)₃ (Alfa, Puratronic) and with anhydrous oxalic acid. Ammonium acetate was obtained from Fisher Scientific. Mohr's salt, (Alfa, Puratronic) was used as the Fe(II) standard. The actinometry was performed in quartz cuvettes or in fluorimetric, polystyrene cuvettes from Dynalab Corp.

Instrumentation and General Procedures. Melting points were determined in capillary tubes using a Thomas Hoover melting point apparatus. Thin-layer chromatography (TLC) was conducted with aluminum plates precoated with silica gel 60-F₂₅₄ (EM Industries). All proton (¹H) and carbon (¹³C) nuclear magnetic resonance (NMR) spectra were recorded on a Varian XL-300 spectrometer. Infrared (IR) spectra were obtained on a Perkin-Elmer 297 spectrometer. Ultraviolet-visible absorption spectra were collected on a Hewlett Packard 8451A diode array spectrophotometer.

All syntheses were conducted under a dry atmosphere of argon. Chromatography refers to flash liquid chromatography according to the method of Still²¹ using 230–400-mesh silica gel 60 (EM Industries). Reverse-phase high-pressure liquid chromatography (HPLC) was conducted on a Dynamax Macro C18 column using a Waters M6000 pump at a flow rate of 9.9 mL/min and a Waters 441 absorbance detector (254 nm).

Syntheses of Inhibitors and Model Compounds. Ethyl (*E*)-*p*-(Diethylamino)-*o*-methoxy- α -methylcinnamate, (*E*)-**5a**. A stirring solution of 4 (923 mg, 3.33 mmol) in THF (50 mL) at room temperature was treated sequentially with a 60% oil dispersion of NaH (225 mg, 5.61 mmol), DMF (7 mL), and CH₃I (0.5 mL, 8.03 mmol),²² at which time the solution was homogeneous. After 20 min, the solvent was removed *in vacuo* and the residue was partitioned between diethyl ether (40 mL) and 10% w/w aqueous NaOH (40 mL). The ether layer was removed, and the aqueous layer was extracted again with diethyl ether (40 mL). The ether layers were combined, washed with brine (10% NaCl), dried over MgSO₄, and concentrated *in vacuo* to produce a liquid which after chromatography (hexane/EtOAc, 90:10) yielded (*E*)-**5a** as a yellow liquid (739 mg, 76%), *R*_f = 0.7 (hexane/EtOAc, 70:30); ¹H NMR (CDCl₃, 300 MHz) δ 1.18 (t, *J* = 7.1 Hz, 6 H), 1.31 (t, *J* = 7.1 Hz, 3 H), 2.08 (d, *J* = 1.3 Hz, 3 H), 3.37 (q, *J* = 7.1 Hz, 4 H), 3.83 (s, 3 H), 4.22 (q, *J* = 7.1 Hz, 2 H), 6.15 (d, *J* = 2.4 Hz, 1 H), 6.26 (dd, *J* = 8.8, 2.4 Hz, 1 H), 7.26 (d, *J* = 8.9 Hz, 1 H), 7.85 (s, 1 H); ¹³C NMR (CDCl₃, 75 MHz) 12.68, 12.74, 14.44, 44.48, 55.30, 60.38, 94.00, 103.30, 112.23, 123.46, 131.31, 134.28, 149.50, 159.47, 169.44; IR (neat) 2960, 1690, 1600, 1550, 1510 cm⁻¹; λ_{max} (MeOH) = 358 nm.

Anal. Calcd for C₁₇H₂₅NO₃: C, 70.07; H, 8.65; N, 4.81. Found: C, 69.80; H, 8.58; N, 4.78.

(*E*)-*p*-(Diethylamino)-*o*-methoxy- α -methylcinnamic Acid, **6**. A solution of (*E*)-**5a** (482 mg, 1.66 mmol) in a mixture of MeOH (4.5 mL)

and 10% w/w aqueous NaOH (4.5 mL) was stirred at 65 °C for 2 h. The reaction flask was cooled (to room temperature) in a water bath. The reaction was titrated with 1 N HCl while being stirred until no more precipitation could be observed occurring in the flask. The slurry was extracted with diethyl ether (30 mL). The acidification and extraction were repeated on the aqueous layer. The ether layers were combined, washed with saturated NH₄Cl, dried over Na₂SO₄, and then concentrated *in vacuo*. After being dried, **6** remained as a bright yellow solid (395 mg, 91%), mp 178–179 °C, *R*_f = 0–0.3 (hexane/EtOAc, 70:30); ¹H NMR (DMSO-*d*₆, 300 MHz) δ 1.11 (t, *J* = 7.0 Hz, 6 H), 1.96 (d, *J* = 1.4 Hz, 3 H), 3.37 (q, *J* = 6.9 Hz, 4 H), 3.79 (s, 3 H), 6.20 (d, *J* = 2.3 Hz, 1 H), 6.27 (dd, *J* = 8.8, 2.4 Hz, 1 H), 7.24 (d, *J* = 8.8 Hz, 1 H), 7.73 (d, *J* = 1.0 Hz, 1 H), 12.0 (s, 1 H); ¹³C NMR (DMSO-*d*₆, 75 MHz) 12.53, 14.24, 43.75, 55.17, 94.01, 103.23, 110.94, 121.91, 130.84, 133.41, 149.36, 159.16, 169.98.

Anal. Calcd for C₁₅H₂₁NO₃: C, 68.42; H, 8.04; N, 5.34. Found: C, 68.25; H, 7.98; N, 5.33.

p-Nitrophenyl (*E*)-*p*-(Diethylamino)-*o*-methoxy- α -methylcinnamate, (*E*)-**5b**. A reaction vessel was charged with **6** (380 mg, 1.44 mmol) and pyridine (7 mL), and the solution was stirred at room temperature. 1,3-Dicyclohexylcarbodiimide (DCC) (360 mg, 1.73 mmol), *p*-nitrophenol (241 mg, 1.73 mmol), and a catalytic amount of 4-(dimethylamino)pyridine (DMAP) were added sequentially to the solution. After 36 h, the reaction mixture was vacuum filtered to remove the precipitate and the filtrate was concentrated *in vacuo*. Two chromatographic efforts (hexane/EtOAc, 80:20 \rightarrow 50:50 and toluene/acetone, 80:20) and drying yielded (*E*)-**5b** as an orange solid (222 mg, 40%), mp 137–138 °C, *R*_f = 0.7 (hexane/EtOAc, 70:30); ¹H NMR (DMSO-*d*₆, 300 MHz) δ 1.13 (t, *J* = 7.0 Hz, 3 H), 2.22 (s, 3 H), 3.41 (q, *J* = 6.9 Hz, 4 H), 3.82 (s, 3 H), 6.22 (d, *J* = 2.1 Hz, 1 H), 6.34 (dd, *J* = 8.8, 2.3 Hz, 1 H), 7.39 (d, *J* = 8.8 Hz, 1 H), 7.49 (dt, *J* = 9.0, 2.0 Hz, 2 H), 8.07 (s, 1 H), 8.30 (dt, *J* = 9.0, 2.0 Hz, 2 H); ¹³C NMR (*d*₆-DMSO, 75 MHz) 12.65, 14.60, 44.53, 55.30, 93.68, 103.51, 111.52, 120.38, 122.73, 122.73, 122.74, 124.99, 125.00, 131.59, 137.47, 145.04, 150.23, 156.68, 159.95, 166.96 ppm; IR (film) 2960, 1710, 1600, 1510 cm⁻¹; FABHRMS *m/z* (MH⁺) calcd for C₂₁H₂₄O₅N₂ 385.1763, found 385.1748 (–4 ppm).

Ethyl (*Z*)-*p*-(Diethylamino)-*o*-methoxy- α -methylcinnamate, (*Z*)-**5a**. A stirring solution of (*E*)-**5a** (37.7 mg) in CH₂Cl₂ (110 mL, eluted through alumina absorption) was photolyzed in a jacketed photolysis apparatus maintained at 0 °C with ice water. The irradiation was conducted with a 450-W Hg Hanovia immersion lamp which was encased in an uranium filter ($\lambda > 330$ nm) and placed in a water-cooled jacketed well. The extent of photoisomerization was monitored by ¹H NMR. Maximum conversion to the *Z* isomer (~35%) was achieved in <3 h of photolysis. Upon removal of the CH₂Cl₂ *in vacuo*, the mixture of *E* and *Z* isomers was separated by preparative reverse-phase HPLC (acetonitrile/H₂O, 80:20). The *Z* isomer was recovered from the HPLC fractions by partially concentrating the fractions *in vacuo*, adding saturated aqueous NaHCO₃ to the remaining liquid, and extracting the aqueous phase twice with diethyl ether. The ether layers were combined, washed with 10% NaCl, dried over Na₂SO₄, and concentrated *in vacuo* to yield (*Z*)-**5a** (9.4 mg, 71% recovery) as a pale, yellow liquid: ¹H NMR (CDCl₃, 300 MHz) δ 1.15 (t, *J* = 7.2 Hz, 3 H), 1.15 (t, *J* = 7.0 Hz, 6 H), 2.05 (d, *J* = 1.5 Hz, 3 H), 3.34 (q, *J* = 7.1 Hz, 4 H), 4.11 (q, *J* = 7.1 Hz, 2 H), 6.10 (d, *J* = 2.4 Hz, 1 H), 6.18 (dd, *J* = 8.7, 2.4 Hz, 1 H), 6.79 (d, *J* = 1.3 Hz, 1 H), 7.09 (d, *J* = 8.6 Hz, 1 H); λ_{max} (MeOH) = 332 nm.

p-Nitrophenyl (*Z*)-*p*-(Diethylamino)-*o*-methoxy- α -methylcinnamate, (*Z*)-**5b**. A stirring solution of (*E*)-**5b** (30 mg) in CH₂Cl₂ (110 mL, previously eluted through alumina) was photolyzed in a jacketed photolysis apparatus which was maintained at 0 °C with ice water. The emission from a 500-W high-pressure Hg lamp (Osram HBO-500 W/2) was passed through an IR filter and a Bausch & Lomb grating monochromator to isolate the 366-nm emission for photolysis. The photoisomerization was monitored by ¹H NMR, which indicated that maximum conversion to the *Z* isomer (~30%) was obtained in <3 h. Upon removal of the CH₂Cl₂ *in vacuo*, the mixture of *E* and *Z* isomers was separated by preparative reverse-phase HPLC (acetonitrile/H₂O, 85:15). The *Z* isomer was recovered from the HPLC fractions by partially concentrating the fractions *in vacuo*, adding water and 10% NaCl to the remaining suspension, and extracting twice with CH₂Cl₂. The CH₂Cl₂ fractions were combined, dried over Na₂SO₄, and concentrated *in vacuo* to yield (*Z*)-**5b** (4.6 mg, 51% recovery) as a pale, yellow film: ¹H NMR (CDCl₃, 300 MHz) δ 1.16 (t, *J* = 7.1 Hz, 6 H), 2.19 (s, 3 H), 3.35 (q, *J* = 7.0 Hz, 4 H), 3.78 (s, 3 H), 6.10 (d, *J* = 2.2 Hz, 1 H), 6.20 (dd, *J* = 8.7, 2.2 Hz, 1 H), 7.06 (s, 3 H), 7.21 (dd, *J* = 8.8, 2.0 Hz, 1 H), 8.19 (d, *J* = 8.8 Hz, 1 H).

(18) A unit refers to an international unit which specifies that 1 μ mol of product is produced per minute for specified conditions.

(19) (a) Parker, C. A. *Proc. R. Soc. London*, **A 1953**, 220, 104. (b) Hatchard, C. G.; Parker, C. A. *Proc. R. Soc. London*, **A 1956**, 235, 518.

(20) Koenigs, P. M. Ph.D. Dissertation, Duke University, 1992.

(21) Still, W. C.; Kahn, M.; Mitra, A. *J. Org. Chem.* **1978**, **43**, 2923.

(22) Stoochnoff, B. A.; Benoiton, N. L. *Tetrahedron Lett.* **1973**, 21.

Isolation of Acyl-Enzymes. The inhibition of chymotrypsin outlined below is similar to that used for thrombin and Factor Xa. An inhibition was performed on a 1.5-mL aliquot of chymotrypsin in Tris buffer (0.5 mg/mL). A methanolic solution of CINN-OpNP, **3a** (1 mg/mL), which required ~1 h of standing, was employed to deliver the inhibitor to the enzyme. Five equivalents of inhibitor were usually used for the inhibition, resulting in a 3–4% methanol concentration in the enzyme sample. Under these conditions, one could expect <5% enzymatic activity in 3 h.

When an inhibited enzyme had reached a constant minimum activity, the stable acyl-enzyme was purified from excess inhibitor by size-exclusion gel chromatography. The filtered sample (0.22- μ m Durapore) was loaded onto the Sephadex column and ~1-mL fractions of eluant were collected in methacrylate disposable cuvettes. The fractions containing the purified acyl-enzyme were identified by monitoring the absorption at 280 and 360 nm, but invariably, the acyl-enzyme eluted in fractions 3–5. The fractions containing the acyl-enzyme were combined and diluted with Tris buffer.

Quantum Yield Determinations under Low-Absorbance Conditions. The light source was a 1000-W high-pressure Hg/Xe lamp (Hanovia 528B-1). It was mounted in a Schoeffel LH 151N lamp housing which was equipped with a Spectral Energy LHC 151/2 condensing lens and a water IR filter with quartz windows. The desired wavelength of irradiation was isolated by a Spectral Energy GM 252 high-intensity grating monochromator. The optical system employed an off-axis Czerny–Turner assembly.²³

Quantum yields for low-absorbance conditions were determined by the method of Zepp.²⁴ Thus, under low-absorbance conditions ($\epsilon l c < 0.12$), the photoreaction will proceed according to first-order kinetics with a rate constant $k = (\ln 10)\Phi I_0 \epsilon L$. If the base-10 extinction coefficient (ϵ , $M^{-1} \text{ cm}^{-1}$) can be determined for the photolyte of interest and the first-order rate constant for the photoreaction can be measured while adhering to the low-absorbance criteria, then the expression $k = (\ln 10)\Phi I_0 \epsilon L$ can be solved for Φ for the relevant experimental conditions. The parameter L is the optical path length, and I_0 is the incident light irradiance (einsteins $L^{-1} s^{-1}$). Excluding the ferrioxalate actinometer, the initial absorbance of all photolyzed solutions was <0.10 at 366 nm.

Determination of ϵ . Quantum yields were measured under low-absorbance conditions, and therefore, the extinction coefficients had to be known for all of the photolytes at the wavelength of irradiation, 366 nm. To determine the extinction coefficient, methods had to be devised to determine the concentration of acyl-enzyme in a purified sample. A general strategy for achieving this end was to measure the absorption of a purified solution, to quantitatively deacylate the enzyme active site, and then to measure the concentration of the coumarin byproduct by UV/vis and fluorescence spectroscopy.²⁰ Previous studies have shown that full enzyme activity is obtained after photoactivation. The product of deacylation, DEAM-coumarin (Scheme II), had a λ_{max} at 380 nm which did not coincide with the proteins' absorption bands, and ϵ_{380} was determined by Beer's law.²⁰

For MeCINN-chymotrypsin, again ϵ_{366} had to be determined for an acyl-enzyme for which purification by size-exclusion gel chromatography resulted in a solution of unknown concentration. For the CINN-enzymes, the absorbance of a purified sample was recorded and then the concentration of acyl-enzyme was determined by photochemically deacylating the acyl-enzyme and quantitating the deacylation product by absorbance. The same strategy was employed for the ϵ_{366} determination of (*E*)-MeCINN-chymotrypsin by invoking hydrolysis as the means of deacylation and by quantitating the hydrolysis product, (*E*)-MeCINN-OH, by absorbance.

The hydrolysis was carried out by adjusting an acyl-enzyme solution to pH > 10. Under these conditions, hydrolysis occurred relatively quickly ($t_{1/2} \approx 2.5$ h). The UV/vis spectrophotometric data which were collected during the course of a hydrolysis displayed an isosbestic point, and the absorbance of an authentic sample of (*E*)-MeCINN-OH under basic conditions did not change over the course of several days.

Quantum Yield Determinations. All photochemical experiments were performed under red lighting. Light irradiances at 366 nm ranged from 4.0×10^{-9} to 2.4×10^{-8} einsteins $L^{-1} s^{-1}$. Quantum yields were determined for a 366-nm irradiation wavelength. Two to four photolyses of a photolyte were conducted between the bracketing ferrioxalate actinometry measurements. A mean value for the quantum yield of the photolyte was obtained from the multiple photolyses of that determination.

Since the solutions adhered to low-absorbance conditions, the photoreactions proceeded according to first-order kinetics. Typically, the

course of reaction was monitored for >8 half-lives to obtain an infinity point. The kinetic data through 3 half-lives was converted to a semi logarithmic plot to obtain the rate constant for photoconversion k . It is essential to maintain rapid and complete mixing throughout the course of the irradiation to maintain a uniform concentration of the chromophore throughout the solution and to insure first-order kinetics. Insufficient mixing results in semilogarithmic first-order kinetic plots that are nonlinear; no such plots were used in this study.

The kinetic data were plotted as $\ln([E]_{\infty} - [E])/([E]_{\infty} - [E]_0)$ vs time (where $[E]$ is the concentration of the enzyme formed in the photoactivation) to obtain the rate constant for photoactivation k from the slope of the plot where $I_0' = I_0$ irradiation volume. The stoichiometry of the photoreaction allows the reaction to be monitored by determining either enzyme or coumarin concentration. The coumarin product is highly fluorescent with 366-nm excitation, but the cinnamates do not fluoresce. Quantum yields were determined by monitoring the first-order increase of DEAM-coumarin fluorescence during photolysis. Thus, photolyses of CINN-OEt were conducted with the excitation beam of the fluorometer, and the extent of photoreaction was monitored continuously and concurrently with photolysis by recording the increase in fluorescence intensity as the reaction progressed.

Photostationary State Experiments. For each geometric isomer of a particular photolyte, a sample was prepared and placed in a quartz cuvette. An absorption spectrum was acquired, and then the sample was photolyzed with 0.5–1-min intervals of 366-nm irradiation. An absorption spectrum was acquired after each period of photolysis, and when the spectra displayed no further change upon irradiation, the photostationary state (PSS) was assumed to have been attained.

For a solution which has been irradiated to photoequilibrium from a pure isomer, the PSS absorbance is proportional to the concentration of original photolyte. Assuming that the same photostationary state is obtained for the photolyses of either isomer, the ratio of the absorbances for the respective photostationary states serves as a correction factor, X , for the difference in concentration between the original solutions of *E* and *Z* photolytes (eq 1). A ratio, R , for the extinction coefficients of the *Z* and *E* isomers is obtained by multiplying the correction factor X by the ratio of absorbances from the pure *E* and *Z* solutions (eq 2).

$$\frac{A_{E \rightarrow \text{PSS}}}{A_{Z \rightarrow \text{PSS}}} = \frac{[E]_{\text{pure}}}{[Z]_{\text{pure}}} = X \quad (1)$$

$$X \frac{A_Z}{A_E} = \frac{\epsilon_Z}{\epsilon_E} = R \quad (2)$$

Once ϵ_Z/ϵ_E has been determined for a chosen wavelength, then the UV/vis spectrophotometric data which are obtained from the photolysis of either isomer can be used to calculate the photostationary state ratio of isomers. For example, the four relationships stated in eqs 3–6 pertain to the photolysis of the *E* isomer to photoequilibrium. These four equations embody the four unknowns ϵ_Z/ϵ_E , $[E]_{\text{pure}}$, $[E]_{\text{PSS}}$, and $[Z]_{\text{PSS}}$; therefore, the four equations can be solved for the PSS ratio $[E]_{\text{PSS}}/[Z]_{\text{PSS}}$ to obtain the expression in eq 7.

$$A_E = \epsilon_E l [E]_{\text{pure}} \quad (3)$$

$$A_{E \rightarrow \text{PSS}} = \epsilon_Z l [Z]_{\text{PSS}} + \epsilon_E l [E]_{\text{PSS}} \quad (4)$$

$$R = \epsilon_Z/\epsilon_E \quad (5)$$

$$[E]_{\text{pure}} = [Z]_{\text{PSS}} + [E]_{\text{PSS}} \quad (6)$$

$$\frac{[E]_{\text{PSS}}}{[Z]_{\text{PSS}}} = \frac{(A_{E \rightarrow \text{PSS}}/A_E) - R}{1 - (A_{Z \rightarrow \text{PSS}}/A_E)} \quad (7)$$

After $[E]_{\text{PSS}}/[Z]_{\text{PSS}}$ has been calculated from data obtained at any appropriate wavelength, knowing ϵ_Z/ϵ_E for the wavelength of irradiation λ_i allows one to obtain a ratio of photoisomerization quantum yields, Φ_Z/Φ_E .

Results

Absorption maxima and extinction coefficients for several acyl-enzymes are presented in Table I.

(23) Strobel, H. A.; Heineman, W. R. *Chemical Instrumentation: A Systematic Approach*, 3rd ed.; Wiley: New York, 1989; p 327.

(24) Zepp, R. G. *Environ. Sci. Technol.* 1978, 12, 327.

Table I. UV/Vis Spectrophotometric Properties of the CINN Photolytes in Tris Buffer (pH 7.4)

photolyte	λ_{\max}	$A_{366}/A_{380} \pm \sigma$ (no. of detms) ^a	ϵ_{366} ^b
CINN-chymotrypsin	372	1.37 \pm 0.01 (7)	25 700
CINN-Factor Xa	358	1.10 \pm 0.01 (3) ^c	20 600
CINN-thrombin	380	1.00 \pm 0.03 (3)	18 600
CINN-OEt	358	1.03 \pm 0.01 (4)	19 200

^a For each solution, A_{366} of the photolyte was measured before irradiation and A_{380} of DEAM-coumarin was measured after irradiation. Standard error is presented as σ ; propagated error is identified as e .^b On the basis of DEAM-coumarin, $\lambda_{\max} = 380$ nm and $\epsilon_{380} \pm \sigma = 18\,274 \pm 360$ M⁻¹ cm⁻¹ (2 detms). ^c In contrast to the other acyl-enzymes where the determinations of A_{366}/A_{380} were made with samples isolated from different gel columns, these three determinations for Factor Xa were made with three different dilutions of sample from one gel column.

Table II. Photoactivation Quantum Yields at 366 nm for CINN-chymotrypsin, CINN-Factor Xa, CINN-thrombin, and CINN-OEt

enzyme	temp (°C)	$\Phi_{E \rightarrow Z} \pm e^{a,b}$
chymotrypsin	10	0.17 \pm 0.03
chymotrypsin	20	0.17 \pm 0.03
chymotrypsin	33	0.17 \pm 0.03
chymotrypsin	room temperature	0.19 \pm 0.04
Factor Xa	10	0.20 \pm 0.02
Factor Xa	20	0.23 \pm 0.03
Factor Xa	33	0.27 \pm 0.02
thrombin	10	0.042 \pm 0.004 ^c
thrombin	20	0.047 \pm 0.004 ^c
thrombin	33	0.042 \pm 0.003 ^c
thrombin	room temperature	0.044 \pm 0.002
CINN-OEt	5	0.13 \pm 0.01
CINN-OEt	20	0.127 \pm 0.004
CINN-OEt	37	0.13 \pm 0.01

^a Mean value of the quantum yield for all determinations at a given temperature. ^b Average quantum yield for all determinations at a given temperature. ^c e = propagated error. ^c These samples scattered a significant amount of light, and the data were corrected for scattering. The correction factor is the ratio of average values of data obtained from filtered and unfiltered solutions ($\Phi_{366\epsilon_{366}}^{\text{filtered}} / (\Phi_{366\epsilon_{366}}^{\text{unfiltered}})$ obtained from non-scattering and scattering samples.

Quantum Yields for the CINN-Enzymes. Isolated CINN-enzymes were photolyzed for known amounts of time, and the extent of reaction was monitored by assaying the production of active enzyme. The first-order kinetic data always displayed good linearity through 3 half-lives upon conversion to a semi-logarithmic plot, and the values of k which were obtained from these plots were used to obtain values of $\Phi_{E \rightarrow Z}$. For each CINN-enzyme, quantum yields were determined at three different temperatures and at various light irradiances. The results are collected in Table II.

The quantum yield at a particular temperature is the average value from determinations made at different light intensities. To judge the sensitivity of $\Phi_{E \rightarrow Z}$ to light irradiance, values of the independent parameter ($\epsilon_{366})(\Phi_{366}) = k/(I_0 L \ln(10))$ at a particular temperature were compared since this accounts for the variability of the irradiation volume among runs. No quantum yield dependency on light intensity was displayed by any of the acyl-enzymes. The light intensity was varied the most for the CINN-thrombin measurements at 20 °C for which the quantum efficiency did not vary over a 6-fold increase in light intensity. Generally, no temperature dependence was displayed by the quantum yields for the CINN-enzymes over a range of 5–37 °C.

Quantum Yields for CINN-OEt. An assessment was to be made of how the active site environments were altering the photochemistry of the cinnamoyl derivative; therefore, $\Phi_{E \rightarrow Z}$ had to be measured for the model compound CINN-OEt. Quantum yields for CINN-OEt were determined and compared to the quantum yields of the CINN-enzymes. Again, a sensitive means of monitoring the photoreaction had to be available to perform the

measurements at the requisite low concentrations of photolyte. The intense fluorescence of the photoproduct DEAM-coumarin served well in this capacity. The rate of photoreaction could be measured by monitoring the increase in fluorescence upon photolysis. The irradiances of the fluorometer beam were similar to the irradiances of the monochromatic illumination system.

Due to the inherent sensitivity of the fluorescence detection method, the experiments were conducted at CINN-OEt concentrations of $\sim 1 \times 10^{-7}$ M. The kinetic data displayed good linearity through 3 half-lives upon conversion to semilogarithmic plots, and quantum yields were calculated from the values of k which were obtained from these plots. The results from measurements at various light irradiances and at three different temperatures were determined, and like the CINN-enzymes, the quantum yield was constant with respect to these variables.

A comparison was to be made between the quantum yields for the CINN-enzymes and for the model compound CINN-OEt, but the data had been acquired with dramatically different techniques. Before basing conclusions on the comparison of the results, we determined the quantum yield of CINN-chymotrypsin with the fluorescence monitoring technique to verify that the same result was obtained with either detection method (coumarin fluorescence or enzymatic activity). The redetermined quantum yield value was within experimental error of those values previously determined.

Photostationary State Determinations. For accurate photostationary state determinations, both the *E* and *Z* isomers of the photolytes had to be obtainable in pure form. (*E*)-MeCINN-OEt (**5a**) and (*E*)-MeCINN-OpNP (**5b**) were easily synthesized. Photolysis ($\lambda > 300$ nm) of either compound as a methylene chloride solution yielded a mixture of isomers which could be separated by reverse-phase HPLC with base-line resolution.

(*E*)- and (*Z*)-MeCINN-OpNP were both inhibitors of chymotrypsin; therefore, the feasibility of the photostationary experiments was contingent upon chymotrypsin recognizing the two new compounds as substrates and upon the subsequently formed acyl-enzymes displaying adequate stability to hydrolysis. Chymotrypsin did react with both (*E*)- and (*Z*)-MeCINN-OpNP. Rates of hydrolysis were acquired for the isomeric acyl-enzymes, and the data indicated that both (*E*)- and (*Z*)-MeCINN-chymotrypsin were stable enough ($\tau_{1/2}$ hydrolysis > 15 h) to be employed for photostationary state comparisons with the corresponding ethyl ester model compounds.

Isolated samples of (*E*)- and (*Z*)-MeCINN-chymotrypsin were photolyzed to obtain the absorbance ratios of $A_{E \rightarrow PSS}/A_E$ and $A_{Z \rightarrow PSS}/A_Z$. An assumption of the PSS experiments was that the same photostationary state mixture was obtained from the irradiation of either isomer. This was supported by the observation that photostationary state mixtures originating from both isomers displayed the same λ_{\max} . Additionally, both isomers of MeCINN-chymotrypsin displayed the same isosbestic point upon photolysis indicating that the photoequilibration of each isomer was occurring between only two states and that they were the same two states for the photolysis of either isomer.

To assess how chymotrypsin's active site was altering the photoequilibrium of MeCINN, PSS experiments were also conducted with the model system MeCINN-OEt. The *Z* isomer of MeCINN-OEt was not readily soluble in Tris buffer, and thus, highly absorbing solutions could only be attained at high methanol cosolvent concentrations (15–20%). The PSS data needed to be reflective of an aqueous system, though, since it was to be compared not only to the MeCINN-chymotrypsin results but also to the previously acquired results for the CINN-photolytes. Therefore, photolyses were conducted for each isomer of MeCINN-OEt at concentrations of the methanol cosolvent varying from 2 to 20%. The ratio $[E]_{PSS}/[Z]_{PSS}$ decreased linearly with increasing concentrations of methanol, so a linear regression analysis was performed on the data to obtain a value for $[E]_{PSS}/$

Table III. Photostationary State Determination for the MeCINN Photolytes in Tris Buffer

photolyte	$[E]_{\text{PSS}}/[Z]_{\text{PSS}} \pm e$	$(\epsilon_Z/\epsilon_E)_{366} \pm e$	$\Phi_{Z \rightarrow E}/\Phi_{E \rightarrow Z} \pm e$
MeCINN-chymotrypsin	1.49 ± 0.02^a	0.55 ± 0.01	2.69 ± 0.04
MeCINN-OEt	0.53 ± 0.01^b	0.31 ± 0.01	1.70 ± 0.03

^a This ratio was calculated from data obtained at 378 nm. ^b This value was obtained from the linear regression analysis for a 5% v/v methanol cosolvent concentration.

Table IV. UV/Vis Spectrophotometric Properties for the MeCINN Photolytes in Various Media

photolyte	medium	λ_{max} (nm)	ϵ_{366} ($\text{M}^{-1} \text{cm}^{-1}$)
(E)-MeCINN-chymotrypsin	Tris buffer	378	$26\,200^a$
(Z)-MeCINN-chymotrypsin	Tris buffer	366	14 600
(E)-MeCINN-OEt	Tris buffer ^b	358	19 000
(Z)-MeCINN-OEt	Tris buffer ^b	332	5900^c
(E)-MeCINN-OEt	methanol	358	$26\,400^d$
(Z)-MeCINN-OEt	methanol	336	9000
(E)-MeCINN-OEt	acetonitrile	356	$25\,700^d$
(Z)-MeCINN-OEt	acetonitrile	334	8400

^a A_{366} (before saponification)/ A_{330} (after saponification) $\pm \sigma = 1.60 \pm 0.02$ (3 detms) for (E)-MeCINN-chymotrypsin. $A_{330} \pm \sigma = 16\,400 \pm 100$ (2 detms) for (E)-MeCINN-OH at pH > 10. ^b 5% methanol cosolvent. ^c $\sigma = \pm 400$ (2 detms). ^d Only one determination made.

$[Z]_{\text{PSS}}$ at a selected, low concentration of cosolvent (5% methanol). The ratio $(\epsilon_Z/\epsilon_E)_{366}$ did not vary over the range of methanol cosolvent; therefore, an average for the ratio was obtained for the data which were collected at all cosolvent concentrations.

The results from the photostationary state determinations for the MeCINN photolytes are collected in Table III. Again, an altering influence of the active site is observed for cinnamoyl photoisomerization as $\Phi_{Z \rightarrow E}/\Phi_{E \rightarrow Z}$ for the derivative increases from 1.70 in solution to 2.69 upon binding to the active site.

MeCINN-OEt in Organic Solvents. To investigate the possibility that the altered photochemical behavior of MeCINN-chymotrypsin might be due simply to a hydrophobic effect, PSS determinations for the model system MeCINN-OEt were conducted in a variety of organic solvents and in water.

The λ_{max} for the isomers and the PSS mixtures of MeCINN-OEt did not vary dramatically with the organic or aqueous media of the solution except for hexane in which a notable blue shift was observed. The ratio of quantum yields $\Phi_{Z \rightarrow E}/\Phi_{E \rightarrow Z}$ was relatively insensitive to different types of organic media with all of the quantum yield ratios falling slightly below unity. However, significantly different photochemical behavior was observed in aqueous media. The data show that the greater value of $\Phi_{Z \rightarrow E}/\Phi_{E \rightarrow Z}$ for MeCINN-chymotrypsin relative to that for MeCINN-OEt in a buffer medium cannot be attributed to the more hydrophobic environment of chymotrypsin's binding site. Actually, $\Phi_{Z \rightarrow E}/\Phi_{E \rightarrow Z}$ for the cinnamoyl derivative decreases to a value close to unity in the surroundings of organic solvents ranging from methanol and acetonitrile (Tables IV–VI) to hexane.

MeCINN-Chymotrypsin under Denaturing Conditions. MeCINN-chymotrypsin and MeCINN-OEt displayed significantly different photochemical behavior, and this difference was attributed to the unique influences which the enzyme active site exerted on the isomerizing moiety. If the attributes of the active site can be held accountable for altering MeCINN photoisomerization, then these manifestations should disappear if the integrity of the active site is destroyed. For example, if protein unfolding exposes MeCINN to bulk solvent, then the "random polypeptide coil" ester of the cinnamoyl derivative should not display photochemical behavior that is any different than that of a simple ester since the enzyme-bound derivative is no longer experiencing the tertiary structure of the active site. In fact, if this depiction is accurate, then achieving various degrees of protein unfolding

should allow one to observe a transition between the values of $\Phi_{Z \rightarrow E}/\Phi_{E \rightarrow Z}$ for MeCINN-chymotrypsin and MeCINN-OEt.

Chemical denaturation is one way to induce protein unfolding, and urea and guanidine hydrochloride are two commonly employed denaturing agents. To document the response of $\Phi_{Z \rightarrow E}/\Phi_{E \rightarrow Z}$ to increasing degrees of protein unfolding, MeCINN-chymotrypsin was incubated in solutions of increasing concentrations of denaturant and these solutions were used for the standard procedure of a PSS determination. Experiments were conducted with both urea and guanidine hydrochloride.

The experimental design necessitated that greater extents of protein unfolding be accompanied by greater exposure of MeCINN to higher concentrations of denaturant. Thus, before any changes which were incurred by $\Phi_{Z \rightarrow E}/\Phi_{E \rightarrow Z}$ could be attributed to loss of the active site's tertiary structure, the response of MeCINN's photochemical behavior to simply the presence of the denaturant needed to be documented.

Photostationary state determinations were performed for MeCINN-OEt in pH 7.4 Tris buffer solutions at concentrations of urea ranging from 0.5 to 8 M and at concentrations of guanidine hydrochloride ranging from 2 to 6 M. High concentrations of denaturant in Tris buffer did not significantly alter the photochemistry of MeCINN-OEt; therefore, any changes in $\Phi_{Z \rightarrow E}/\Phi_{E \rightarrow Z}$ upon MeCINN-chymotrypsin denaturation could be attributed to loss of the active site's tertiary structure.

A protein requires a finite amount of time to reestablish equilibrium (*i.e.*, unfold) after being placed in a destabilizing environment.^{25–28} A knowledge of the time frame for MeCINN-chymotrypsin denaturation was necessary to allocate the time which would be required by an acyl-enzyme to incubate in a denaturant before photolysis was conducted for the PSS determination. (E)-MeCINN-chymotrypsin was isolated and incubated in 8 M urea or 6 M guanidine hydrochloride. The ratio $A_{E \rightarrow \text{PSS}}/A_E$ was monitored to follow the extent of protein unfolding with respect to time. As prescribed by these results, isomers of MeCINN-chymotrypsin were allowed to incubate for 1 h in urea solutions and for 10 min in guanidine hydrochloride solutions before photolyses were conducted for the PSS determinations. The results of the PSS experiments correspond well to the results of other chymotrypsin denaturation studies in urea and guanidine hydrochloride for which active site probes were used to monitor the extent of protein unfolding.^{28,29} The enzyme's influence on the cinnamoyl photochemistry disappears concurrently with the loss of the active site's tertiary structure (Figure 1).

Interestingly, the values of $\Phi_{Z \rightarrow E}/\Phi_{E \rightarrow Z}$ at the highest denaturant concentrations overshoot the value for MeCINN-OEt in Tris buffer and approach the values for MeCINN-OEt in organic solvents. This result suggests that the cinnamoyl derivative experiences a more hydrophobic environment when its ester linkage is a "random-coil" protein than when it exists as a simple alkyl ester. This interpretation is consistent with studies on the charge-transfer ability of aromatic side chains in denatured proteins, the results of which indicate that incomplete exposure of the aromatic residues to the solvent environment is at least partially due to the statistical fluctuations of the mobile, randomly coiled polypeptide.³⁰ The acyl-enzyme value of 1.42 to $\Phi_{Z \rightarrow E}/\Phi_{E \rightarrow Z}$ in 6 M guanidine hydrochloride more closely resembles the MeCINN-OEt value in Tris buffer (1.70) than does the acyl-enzyme value of 1.14 in 8 M urea. This may be indicative of the different mechanisms by which the two denaturants operate;

(25) Gerig, J. T.; Halley, B. A. *Arch. Biochem. Biophys.* **1981**, *209*, 152.

(26) Hopkins, T. R.; Spikes, J. D. *Biochem. Biophys. Res. Commun.* **1967**, *28*, 480.

(27) Tsou, C. L. *Asia Pac. Commun. Biochem.* **1987**, *1*, 157.

(28) Morrisett, J. D.; Broomfield, C. A. *J. Am. Chem. Soc.* **1971**, *93*, 7297.

(29) Berliner, L. J. *Biochemistry* **1972**, *11*, 2921.

(30) Coan, C. R.; Hinman, L. M.; Deranleau, D. A. *Biochemistry* **1975**, *14*, 4421.

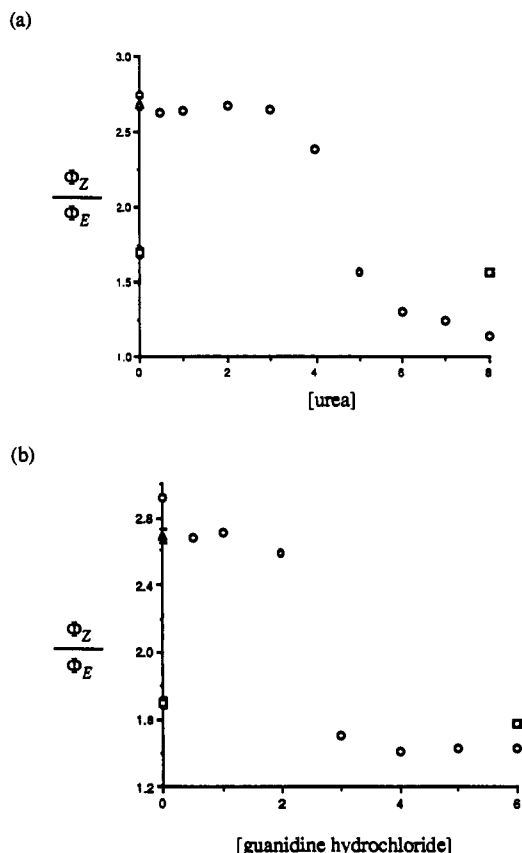


Figure 1. $\Phi_{Z \rightarrow E}/\Phi_{E \rightarrow Z}$ for MeCINN-chymotrypsin as a function of chemical denaturation. The ratio $[E]_{PSS}/[Z]_{PSS}$ was calculated from data collected at 378 nm: (a) urea in Tris buffer; (b) guanidine hydrochloride in Tris buffer; O, values from denaturation experiments; Δ , previously determined value; and \square , values from MeCINN-OEt.

supposedly, urea establishes more hydrophobic contacts with the protein residues than does guanidine hydrochloride.^{29,31}

Photoisomerization Quantum Yields for MeCINN-chymotrypsin and for MeCINN-OEt. Since values of $(\epsilon_Z/\epsilon_E)_{366}$ had already been obtained for the MeCINN photolytes from the photostationary state determinations, ϵ_{366} had to be determined outright for only one isomer of each geometric pair. The insolubility of (*E*)-MeCINN-OEt in Tris buffer precluded the preparation of solutions at accurate concentrations. Thus, preparative quantities of the intrinsically more soluble *Z* isomer were isolated, and its ϵ_{366} was determined by conventional means. Likewise, the extinction coefficients for (*E*)-MeCINN-OEt in methanol and acetonitrile were measured according to standard procedures.

Since the MeCINN photolytes were irradiated under low-absorbance conditions, the approach to the photostationary state proceeded according to first-order kinetics and the system could be treated as a simple first-order approach to equilibrium (eqs 8 and 9)

$$d[E]/dt = k_{E \rightarrow Z}[E] - k_{Z \rightarrow E}([E]_0 - [E]) \quad (8)$$

$$\ln \frac{([E]_0 - [E]_{PSS})}{[E] - [E]_{PSS}} = k_{PSS}t \quad (9)$$

where $k_{PSS} = k_{E \rightarrow Z} + k_{Z \rightarrow E} = (\ln 10)\Phi_{E \rightarrow Z}I_0\epsilon_ZL + (\ln 10)\Phi_{Z \rightarrow E}I_0\epsilon_ZL$.

Measuring the rates of approach to the photostationary state and having already determined $\Phi_{Z \rightarrow E}/\Phi_{E \rightarrow Z}$ in the photostationary state experiments, $\Phi_{E \rightarrow Z}$ and $\Phi_{Z \rightarrow E}$ could be solved uniquely for each photolyte under specified conditions.

(31) Hibbard, L. S.; Tulinsky, A. *Biochemistry* **1978**, *17*, 5460.

Table V. Photoisomerization Quantum Yields at 366 nm for the MeCINN Photolytes in Various Media

photolyte	medium	$\Phi_{E \rightarrow E} + \Phi_{Z \rightarrow Z} \pm \sigma$ ($M^{-1} cm^{-1} \times 10^{-3}$) (no. of detms)	Φ
(<i>E</i>)-MeCINN-chymotrypsin	Tris buffer		0.065 ± 0.01^a
(<i>Z</i>)-MeCINN-chymotrypsin	Tris buffer	4.26 ± 0.43 (8)	0.17 ± 0.02^b
(<i>E</i>)-MeCINN-OEt	Tris buffer	4.18 ± 0.33 (7)	0.14 ± 0.01^a
(<i>Z</i>)-MeCINN-OEt	Tris buffer		0.24 ± 0.02^b
(<i>E</i>)-MeCINN-OEt	MeOH	11.9 ± 0.5 (6)	0.34^a
(<i>Z</i>)-MeCINN-OEt	MeOH		0.33^b
(<i>E</i>)-MeCINN-OEt	CH ₃ CN	13.1 ± 0.3 (7)	0.39^a
(<i>Z</i>)-MeCINN-OEt	CH ₃ CN		0.37^b

^a $\Phi_{E \rightarrow Z}$. ^b $\Phi_{Z \rightarrow E}$.

UV/vis spectrophotometry was the only convenient means to monitor the extent of photoreaction. The kinetic data always displayed linearity through 3 half-lives upon conversion to a semilogarithmic plot, and the values of k_{PSS} from these plots were used for the quantum yield calculations. The results are collected in Table V.

Discussion

We speculate that two effects must be considered that alter cinnamate photochemistry in the enzyme active site. First, the active site apparently enforces planarity on the cinnamate, and this affects the absorbance of the chromophore and the efficiency of its photoprocesses. The size of the cinnamate is also important in this steric enforcement, and increasing the size of the cinnamate by addition of a methyl group (CINN vs MECINN) results in an even greater restriction. Second, protic acids in the active site may alter the photoefficiency of isomerization by serving as catalysts for excited-state processes.

The λ_{max} of the CINN moiety is red-shifted to differing extents relative to CINN-OEt when it is bound to the three unique protein environments of chymotrypsin, Factor Xa, and thrombin (Table I). Typically, acyl-enzyme intermediates of serine proteases do exhibit red shifts in their absorption maxima relative to those of ester model compounds.³² The origin of this red shift has been investigated with resonance Raman spectroscopy on (*p*-(dimethylamino)benzoyl)chymotrypsin and (*p*-(dimethylamino)cinnamoyl)chymotrypsin by Peticolas and co-workers.³³⁻³⁵ The conclusion was reached that the λ_{max} shift of (*p*-(dimethylamino)benzoyl)chymotrypsin was not due to the "effective" solvent environment of the enzyme active site but rather that the acyl moiety of (*p*-(dimethylamino)benzoyl)chymotrypsin had an electronic configuration which more closely resembled that of an aldehyde than that of an ester.

The crystal structure of CINN-chymotrypsin¹⁷ supports the notion that a portion of the red shift for the CINN chromophore of this acyl-enzyme (372 vs 358 nm for the ethyl ester) arises from a more "aldehyde-like" binding mode within the active site than from the *s-cis* or *s-trans* conformation of a typical ester. The dihedral angle about $O_{C=O}-C_{C=O}-O_{\gamma-Ser}-C_{\beta-Ser}$ of the acyl linkage is 64.7° , significantly deviating from planarity. The crystal structure also suggests other features of the acyl-enzyme which may contribute to the protein-induced red shift of the cinnamoyl derivative.

The crystal structure of CINN-chymotrypsin indicates that the cinnamoyl derivative is completely planar with the exception

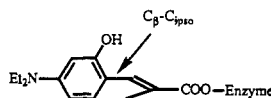
(32) (a) Bernhard, S. A.; Lau, S. J. *Cold Spring Harbor Symp. Quant. Biol.* **1971**, *36*, 75. (b) Bernhard, S. A.; Malhotra, O. P. *Isr. J. Chem.* **1974**, *12*, 471.

(33) Argade, P. V.; Gerke, G. K.; Weber, J. P.; Peticolas, W. L. *Biochemistry* **1984**, *23*, 299.

(34) Weber, J. A.; Turpin, P.; Bernhard, S. A.; Peticolas, W. L. *Biochemistry* **1986**, *25*, 1912.

(35) Jaffé, H. H.; Orchin, M. *Theory and Applications of Ultraviolet Spectroscopy*; Wiley: New York, 1962.

of the alkyl groups on the diethylamino substituent. The torsional angles of the enone double bond are -1.9° for $C_{\text{ipso}}-C_\beta-C_\alpha-C_{\text{CH}_3}$ and -177.8° for $C_{\text{ipso}}-C_\beta-C_\alpha-C_{\text{C=O}}$. We suggest that inhibition to twisting about the $C_{\text{ipso}}-C_\beta$ single bond could be contributing to the red shift of the acyl enzyme. In solution, CINN-OEt experiences a torsional twist about $C_{\text{ipso}}-C_\beta$ of $\sim 40^\circ$ to relieve steric repulsion between the α -methyl group and the phenyl ring.^{36,37} Crystalline CINN-chymotrypsin displays torsional angles of 179.8° and 3.6° from the two *o*-phenyl carbons through the α -carbon. The geometrical constraints of the active site apparently bestow greater planarity to CINN's conjugated system relative to the solution conformation of the ethyl ester. Increased planarity enhances conjugation which would contribute to the red shift of the chromophore upon binding to the chymotrypsin active site.



Electrostatic interactions between CINN and charged protein moieties must also be considered as potential contributors to a protein-induced red shift of the chromophore.³⁸ The crystal structure of CINN-chymotrypsin suggests a weak interaction between the diethylamino nitrogen and the backbone carbonyl oxygen of residue 217. A distance of 1.89 \AA separates the two atoms in the crystal. The oxygen would possess a partial negative charge from the ionic resonance contribution of the amide functionality. The carbonyl of the CINN moiety resides in a position which would typically be occupied by the nitrogen of an amide linkage undergoing hydrolysis in enzymatic catalysis. Thus, the CINN carbonyl oxygen is in close proximity to ϵN of His 57 (2.1 \AA), and the crystal structure indicates that ϵN is protonated and that His 57 carries a positive charge.

The UV/vis spectral characteristics of CINN-Factor Xa are interesting because the enzyme active site appears to be exerting no influence on the chromophore's electronic properties. CINN-Factor Xa and CINN-OEt have the same λ_{max} (358 nm) for which the extinction coefficients are not significantly different. Although the active site environment certainly presents a different effective solvent environment to the chromophore, no absorption-altering geometrical constraints or electrostatic interactions seem to be imposed upon the chromophore by the protein environment. On the other hand, CINN-thrombin has the greatest perturbation of the chromophore's electronic properties (380 nm). Unfortunately, crystal structures of CINN-thrombin and CINN-Factor Xa have not been solved, and the differences between these acyl-enzymes and CINN-chymotrypsin cannot be discussed at the structural level.

For the quantum yield determinations reported here, rates were measured for enzymatic photoactivation and for coumarin formation (step 2 in Scheme II, b). The proposed mechanism of CINN photoreaction consists of the two consecutive, unimolecular reactions of photoisomerization and subsequent thermal lactonization. Although the quantum yield experimental design only provided a means of measuring the overall process of the two combined steps, clean first-order kinetic behavior was always displayed by these systems. Rate constants for photoactivation and coumarin formation ranged from 1.7×10^{-3} to $2.5 \times 10^{-2} \text{ s}^{-1}$ in the quantum yield determinations. Rate constants for lactonization which had been independently determined³⁹ ranged from $(1.7 \text{ to } 4.6) \times 10^3 \text{ s}^{-1}$. Thus, under the experimental conditions, photoisomerization was the rate-determining step of

photoactivation (or coumarin formation), and therefore, the acquired kinetic data unambiguously reflect a quantum yield for the rate-limiting photoisomerization step.

Structural and spectroscopic evidence for the CINN-enzymes indicated that a protein constraint could enforce greater planarity to the conjugated system when it was bound to an enzyme than when it was free in solution. A force which constrains the chromophore to one plane could be visualized as also opposing the motion of isomerization, resulting in a decrease of the photoisomerization efficiency for the cinnamoyl derivative when it was bound at the enzyme active site. While the quantum yield for CINN-thrombin (0.044) was one-third of that for CINN-OEt (0.13), CINN-Factor Xa photoisomerized with an efficiency that was almost twice this value (0.23), and $\Phi_{E \rightarrow Z}$ for CINN-chymotrypsin was also greater than $\Phi_{E \rightarrow Z}$ for the model compound. Obviously, other factors of the active site environment need to be considered, which could result in an enhancement of *trans* to *cis* photoisomerization.

Lewis *et al.* demonstrated that addition of a Lewis acid to methyl cinnamate isomers enhanced $\Phi_{E \rightarrow Z}$ while $\Phi_{Z \rightarrow E}$ was unaffected. Additionally, in the presence of a Lewis acid, $\Phi_{E \rightarrow Z}$ and $\Phi_{Z \rightarrow E}$ for the methyl cinnamates summed to one, suggesting that no decay occurred from the initial excited states and that all excited molecules relaxed to a common intermediate. Coordination of the Lewis acid to the carbonyl of the *trans* isomer could possibly lower the polar energy barrier leading to the perpendicular state. Brønsted acids have also been employed to enhance *trans* to *cis* photoisomerizations of α,β -unsaturated carbonyl compounds.⁴⁰

We suggest that within the enzyme active site, an advantageously placed proton-donating functionality could coordinate to the carbonyl oxygen of an isomerizing CINN moiety, thus lowering the energy barrier for twisting to the charge-separated intermediate. A lower energy barrier for twisting could be manifested in a greater isomerization quantum yield, and this possibility could explain why an enhanced quantum yield was observed for CINN-Factor Xa and CINN-chymotrypsin relative to that for CINN-OEt.

The chymotrypsin active site presents several possible sites where polar interactions with CINN's carbonyl could occur. A distance of 2.1 \AA separates the ϵ nitrogen of His 57 and the oxygen of CINN's carbonyl.¹⁷ The carbonyl oxygen occupies a position which during normal catalysis accommodates the nitrogen of the amide linkage undergoing hydrolysis. In the crystal structure, the ϵ nitrogen of His 57 is protonated, and the side chain possesses a positive charge. If this situation prevails in solution, then His 57 could serve as a hydrogen-bond donor to the isomerizing cinnamoyl derivative since during normal catalysis ϵN of His 57 is capable of transferring a proton to the amine leaving group of a substrate. An equally viable site for stabilization of an isomerizing CINN moiety is the so-called oxyanion hole (amide N-Hs in the active site that stabilize developing negative charge on the carbonyl oxygen).

To address the question of how the enzyme active site affects CINN photochemistry, we sought a system where both *E* to *Z* to *E* isomerization could be examined. Thus, with the intention of not significantly altering the electronic nature of the CINN moiety, the *o*-hydroxy was methylated for the acyl-chymotrypsin photolyte and the corresponding ethyl ester model compound. A summary of the photophysical and photochemical parameters for the CINN and MeCINN photolytes is presented in Table VI. The quantum yields of 0.14 for (*E*)-MeCINN-OEt and of 0.13 for CINN-OEt agree within experimental error; therefore, the methyl group apparently does not intrinsically perturb the photochemistry of the cinnamoyl derivative. However, the interaction of the additional methyl group within the active site of chymotrypsin does significantly alter the enzymic system. A

(36) Sandris, C. *Tetrahedron* **1968**, *24*, 3569.

(37) Bryan, R. F.; White, D. H. *Acta Crystallogr., Sect. B* **1982**, *B38*, 1332.

(38) (a) Warshel, A.; Levitt, M. *J. Mol. Biol.* **1976**, *103*, 227. (b) Warshel, A.; Weiss, R. M. *J. Am. Chem. Soc.* **1980**, *102*, 6218.

(39) Porter, N. A.; Bruhne, J. D. *J. Am. Chem. Soc.* **1989**, *111*, 7616.

(40) Childs, R. F. *Rev. Chem. Intermed.* **1980**, *3*, 285.

Table VI. Summary of Photophysical and Photochemical Data for the CINN and MeCINN Photolytes at 20 °C

photolyte	medium	ϵ_{366} (M ⁻¹ cm ⁻¹)	λ_{\max} (nm)	Φ	$\frac{\Phi_{Z \rightarrow E}}{\Phi_{E \rightarrow Z}}$
CINN-chymotrypsin	Tris buffer	25 700	372	0.17 ^a	
CINN-Factor Xa	Tris buffer	20 600	358	0.23 ^a	
CINN-thrombin	Tris buffer	18 600	380	0.044 ^a	
CINN-OEt	Tris buffer	19 200	358	0.13 ^b	
(<i>E</i>)-MeCINN-chymotrypsin	Tris buffer	26 200	378	0.06 ^c	2.7
(<i>Z</i>)-MeCINN-chymotrypsin	Tris buffer	14 600	366	0.17 ^d	
(<i>E</i>)-MeCINN-OEt	Tris buffer	19 000	358	0.14 ^c	1.7
(<i>Z</i>)-MeCINN-OEt	Tris buffer	5900	332	0.24 ^d	
(<i>E</i>)-MeCINN-OEt	MeOH	26 200	358	0.34 ^c	0.99
(<i>Z</i>)-MeCINN-OEt	MeOH	9000	336	0.33 ^d	
(<i>E</i>)-MeCINN-OEt	CH ₃ CN	25 700	356	0.39 ^c	0.94
(<i>Z</i>)-MeCINN-OEt	CH ₃ CN	8400	334	0.37 ^d	

^a Quantum yield for photoactivation; all quantum yields at 366 nm.

^b Quantum yield for photolactonization. ^c Quantum yield for *E* → *Z*.

^d Quantum yield for *Z* → *E*.

quantum yield of 0.06 for (*E*)-MeCINN-chymotrypsin is appreciably less than the quantum yield of 0.17 for CINN-chymotrypsin. The altered photochemical behavior of MeCINN-chymotrypsin is unambiguously attributed to the active site's tertiary structure. The value of $\Phi_{Z \rightarrow E}/\Phi_{E \rightarrow Z}$ for MeCINN-

chymotrypsin is 2.69 whereas the ratio for MeCINN-OEt is 1.70. Upon chemical denaturation, the acyl-enzyme value undergoes a transition toward the MeCINN-OEt value concurrently with protein unfolding in the active site region. Inspection of the X-ray crystal structure of CINN-chymotrypsin shows that a methyl group attached to the *o*-hydroxyl group would place that methyl carbon within 2 Å of residues 214–216 of the protein and within 3.5 Å of residues 190–194. The additional methyl clearly causes an already crowded active site to be further hindered.

The UV/vis spectral data of the CINN photolytes can be used as a gauge of the geometrical constraints which were imposed upon the chromophores by the enzyme active sites. Particularly, a contribution to the red shift was attributed to the apparent ability of the active sites to impose planarity to the conjugated systems. The magnitude of this effect correlates with the photoisomerization efficiencies of the bound moieties. For example, among the (*E*)-acyl-enzymes, the ones which displayed the greatest red shifts from their model compounds also exhibited the most inefficient photochemistry (Table VI, first 3 entries). The same force which imposes planarity to a conjugated system also appears to hinder the requisite motion for photoisomerization.

Acknowledgment. N.A.P. gratefully acknowledges support of this research from NIH (HL 17921). P.M.K. acknowledges support from an NIH Pharmacology Training Grant.